Conduction velocity is regulated by sodium channel inactivation in unmyelinated axons innervating the rat cranial meninges

Roberto De Col, Karl Messlinger and Richard W. Carr

Institute for Physiology and Pathophysiology, University of Erlangen-Nuremberg, Erlangen, Germany

Axonal conduction velocity varies according to the level of preceding impulse activity. In unmyelinated axons this typically results in a slowing of conduction velocity and a parallel increase in threshold. It is currently held that Na^+–K^+-ATPase-dependent axonal hyperpolarization is responsible for this slowing but this has long been equivocal. We therefore examined conduction velocity changes during repetitive activation of single unmyelinated axons innervating the rat cranial meninges. In direct contradiction to the currently accepted postulate, Na^+–K^+-ATPase blockade actually enhanced activity-induced conduction velocity slowing, while the degree of velocity slowing was curtailed in the presence of lidocaine (10–300 μM) and carbamazepine (30–500 μM) but not tetrodotoxin (TTX, 10–80 nM). This suggests that a change in the number of available sodium channels is the most prominent factor responsible for activity-induced changes in conduction velocity in unmyelinated axons. At moderate stimulus frequencies, axonal conduction velocity is determined by an interaction between residual sodium channel inactivation following each impulse and the retrieval of channels from inactivation by a concomitant Na^+–K^+-ATPase-mediated hyperpolarization. Since the process is primarily dependent upon sodium channel availability, tracking conduction velocity provides a means of accessing relative changes in the excitability of nociceptive neurons.

(Received 24 September 2007; accepted 14 December 2007; first published online 20 December 2007)
Corresponding author R. W. Carr: Department of Physiology, University of Munich, Pettenkoferstrasse 12, D-80336 Munich, Germany. Email: richard.carr@med.uni-muenchen.de

The speed of action potential conduction in individual axons varies according to the level of preceding activity. For neurons with unmyelinated axons, a considerable proportion of which are nociceptive, repetitive activation typically results in a progressive slowing of conduction velocity (Thalhammer *et al.* 1994), an increase in the minimum charge required for electrical activation (Raymond, 1979) and the possibility of conduction failure (Weidner *et al.* 2003). The slowing of axonal conduction velocity in response to activity can therefore be considered as an intrinsic means of self-inhibition in umyelinated axons.

Activity-induced changes in conduction velocity are relatively homogeneous amongst sensory neurons of the same receptive sensory class and this index has therefore found use primarily in fibre classification (Thalhammer *et al.* 1994; Gee *et al.* 1996; Weidner *et al.* 1999; Serra *et al.* 1999; Campero *et al.* 2004). For multi-unit microneurographic recordings of human unmyelinated C-fibres, activity-induced changes in conduction velocity also form the basis of the 'marking' technique employed to identify periods of activity in single unmyelinated axons. Recent microneurographic evidence suggests that conduction velocity slowing profiles are altered in single axons from neuropathic patients (Orstavik *et al.* 2003, 2006) and changes in both basal conduction velocity (Djouhri & Lawson, 2001) as well as the slowing profiles of unmyelinated axons have also been reported in animal models of chronic injury (Shim *et al.* 2007). However, the interpretation of such changes has been precluded by a lack of understanding of the fundamental mechanism responsible for activity-induced changes in axonal conduction velocity.

In principal, the speed of action potential propagation is determined by the rate at which the membrane capacity is discharged by the sodium action current. Changes in conduction velocity within an individual neuron could therefore result from changes in (1) the magnitude and kinetics of the active sodium current, (2) the total membrane conductance, (3) membrane potential or some combination of the three. Since it is well established that action potential activity is accompanied by a Na^+–K^+-ATPase-dependent axonal hyperpolarization (Rang & Ritchie, 1968; Gordon *et al.*

 DOI: 10.1113/jphysiol.2007.145383

1990; Morita *et al.* 1993; Kobayashi *et al.* 1997) this has hitherto been assumed causal for activity-induced reductions in conduction velocity. This idea has been consolidated by intra-axonal recordings from lizard motoneurons demonstrating that post-activity hyperpolarization is primarily mediated by Na^+–K^+-ATPase activity and furthermore that the hyperpolarization is not obligatorily associated with any change in total membrane conductance (Morita *et al.* 1993). However, changes in the active sodium current can also occur without affecting membrane conductance and thereby offer an alternative, plausible mechanism whereby conduction velocity can be modulated during repetitive activity (Bliss & Rosenberg, 1979). Presently though, methods to examine this process directly in single unmyelinated axons have not been realized but, in small dorsal root ganglion (DRG) somata, a cumulative inactivation of sodium currents results from both repetitive brief depolarizing steps as well as repetitive action potential voltage profiles (Blair & Bean, 2003; Tripathi *et al.* 2006).

To investigate the candidate mechanisms contributing to conduction velocity changes in response to repetitive activity in single unmyelinated axons, a rat cranial dura mater preparation was established. A significant advantage of the cranial dura is that the distal portion of sensory axons innervating it are only scantily encased in perineurium (Andres *et al.* 1987). This allows good pharmacological access to the nerve terminal and a substantial length of axon proper. Using this preparation we have investigated the role of Na^+–K^+-ATPase activity, intracellular Na^+ accumulation and sodium channel inactivation on activity-induced changes in the conduction velocity of single unmyelinated axons.

Methods

Animal housing and all experimental procedures were carried out in compliance with the guidelines for the welfare of experimental animals as stipulated by the Federal Republic of Germany.

Tissue preparation

Wistar rats of both sexes and with body weights ranging from 250 to 370 g were used. Rats were killed by placing them in a carbon dioxide atmosphere. The head and lower jaw were removed and the cranial vault cleared of all overlying skin and muscle. The skull was divided mid-sagittally with a scalpel. The cortex and brainstem were gently lifted out of each of the resulting skull halves, exposing the underlying dura. One skull half was embedded in agar inside a perspex chamber such that the dura-lined skull itself formed a tissue bath. The second skull half was kept in buffered physiological solution at room temperature. The intervening period before use of the second half-skull was typically less than 4 h and no differences in average conduction velocity or the average magnitude of slowing were found between axons innervating the two halves.

The tissue was perfused continuously at *ca* 5 ml min^{-1} with physiological solution of the following composition (mM): 145 Na^+; 3.5 K^+, 1.53 Ca^{2+}, 0.69 Mg^{2+}; 1.67 PO_4^{2-}; 114 Cl^-; 9.64 $C_6H_{11}O_7$; 5.55 D(+)-glucose; 7.6 D(+)-sucrose and was buffered to pH 7.4 with carbogen (95% O_2–5% CO_2). The temperature of the perfusing solution was controlled with a flow-through Peltier element regulated by feedback from a thermocouple positioned in the bath, close to the dura. Typically the preparation was held at $35.5 \pm 0.5^\circ$C. In those experiments in which the effects of temperature on activity-induced slowing were studied the control bath temperature was $32.0 \pm 0.5^\circ$C such that a 6°C warming did not encroach on the activation range of heat sensitive fibres.

Recording arrangement

A nerve, comparable to the spinosus nerve in humans and innervating a large portion of the parietal and temporal cranial meninges, was identified and cut distal to its point of entry into the trigeminal nerve. The distal cut end was freed of surrounding tissue over a length of approximately 4 mm. A glass recording electrode, filled with physiological solution and with a tip diameter of *ca* 10 μm, was attached to the side of the isolated nerve stem by light suction (Fig. 1*A*). Single unit receptive fields were located by repeated random placements of the electrode onto the dura until a single 'all-or-none' action potential could be readily distinguished by its constant latency response to electrical stimulation (see Fig. 1*C*). Signals were filtered (5 kHz low-pass), amplified (Axopatch 200A, Axon Instruments, USA), digitized (micro 1401, Cambridge Electronic Design, UK) and stored to disk for later processing with custom written software in Igor Pro (Wavemetrics, USA).

Unit identification and stimulation

A custom-built electrode was used to deliver constant current stimuli within a unit's electrical receptive field. A standard electrical stimulation protocol was used to characterize units. This consisted of a 300 s pause followed by stimulation at 2 Hz for 180 s and a subsequent 600 s period of stimulation at 0.5 Hz. The singularity of each unit was confirmed by (a) the consistency of its latency to electrical stimulation at low frequency, (b) the consistency of spike shape (Fig. 1*C* inset) and (c) a non-discontinuous trajectory of latency changes in response to a constant

frequency of stimulation (see Fig. 1*E*). All axons reported here had conduction velocity slowing profiles that were well fitted by either a single or double exponential function.

The distinction between efferent autonomic and afferent insensitive axons is equivocal particularly in *ex vivo* tissue preparations. Consequently, the electrophysiological criterion developed in humans for the identification of sympathetic axons (Campero *et al.* 2004) was used to exclude some axons. Specifically, in response to electrical stimulation at 2 Hz for 180 s, those axons that showed a period of relative conduction velocity speeding after an initial slowing were deemed to be sympathetic and excluded from the dataset. When recording conditions permitted, responsiveness to capsaicin (1 μM) or mechanical or thermal stimulation was also tested. The response of a unit to either one or more of these stimuli demonstrated unequivocally that the axon was afferent. For those axons that were not tested with any sensory stimuli or that did not respond to any of the stimulus modalities, the possibility that these axons were of autonomic origin cannot be excluded.

Changes in bath temperature were achieved by either heating or cooling the fluid entering the bath at a rate

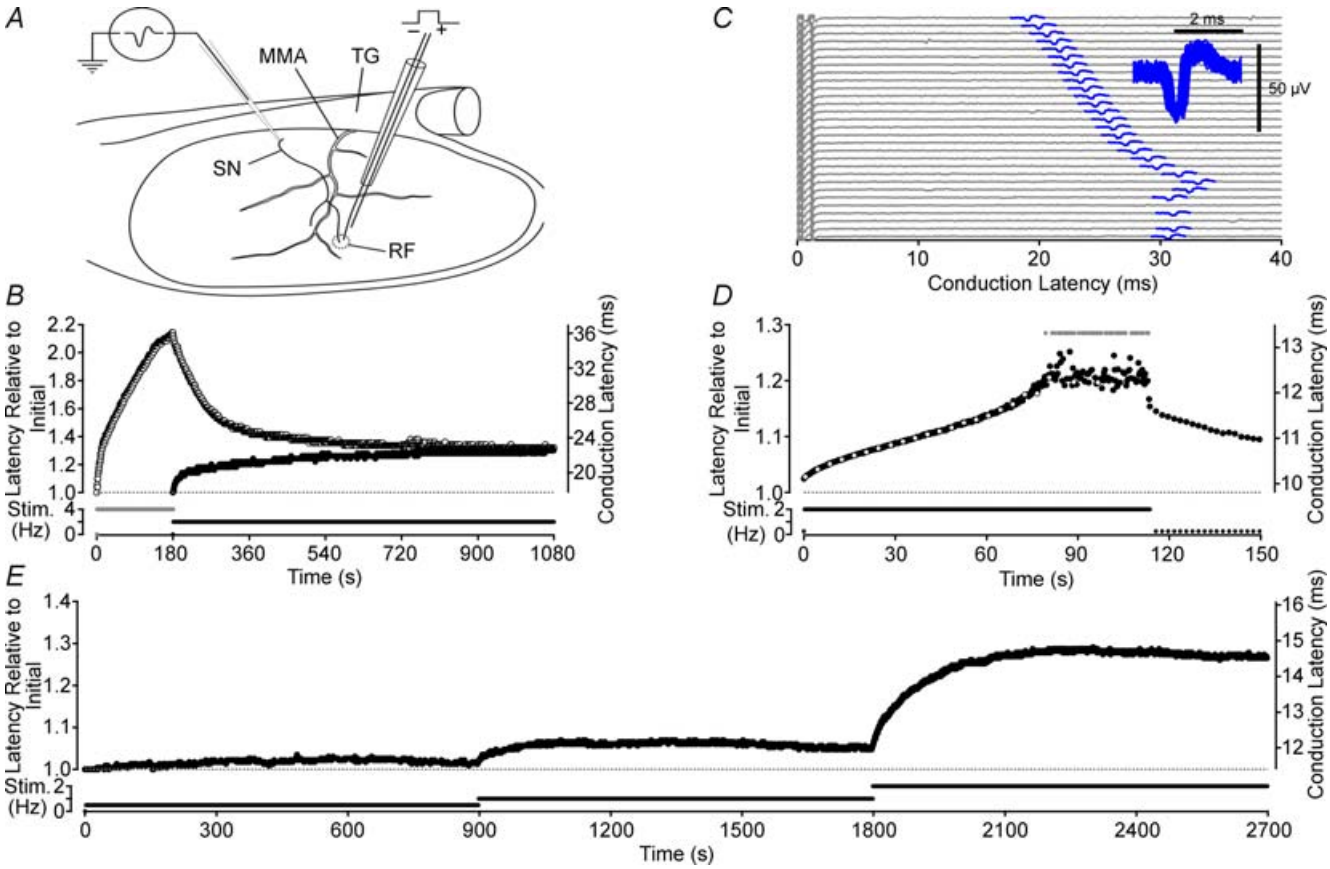

Figure 1. Features of activity-induced changes in conduction latency
Deriving from somata in the trigeminal ganglion (TG), the spinosus nerve (SN) branches from the trigeminal nerve and enters the skull recurrently accompanying the medial meningeal artery (MMA) briefly before branching to innervate the meninges (*A*). A loose patch recording from the SN allows action potentials (*C*, inset) in single axons to be discerned by a consistency of spike shape (*C*, 100 spikes overlaid) and a constant latency response to electrical stimulation in their receptive field (RF). Repetitive electrical stimulation alters conduction velocity, measured as latency, in a frequency-dependent manner. For each stimulus frequency a corresponding steady-state conduction latency is approached from both an initially shorter latency (●, *B*) as well as from longer latencies, induced with a brief period of higher frequency stimulation (○, *B*). When stimulated at a sufficiently high rate, conduction latency progressively increases until a point is reached at which some stimuli fail to evoke an action potential response (grey symbols indicate no response, *D*; lower sweeps in *C*). The open symbols on every sixteenth sweep in *D* correspond to the raw data sweeps shown in *C*. As failures begin to occur the variance of the response latency increases (*C* and *D*) and we have termed this point the 'critical deficit' latency, a latency beyond which conduction is stochastic (see Discussion). For frequencies of stimulation below those bringing the fibre to the critical deficit latency, the relationship between stimulus frequency and steady-state conduction latency is monotonic positive (*E*).

of $\sim 0.1^{\circ}\mathrm{C\,s^{-1}}$ to the target temperature. The new bath temperature was held stabile for at least 10 min before responses to electrical stimulation were examined. The stimulation procedure for each experimental protocol was the same as that used for the control fibre characterization (see above). For the application of substances, an initial wash-in period of no less than 3 min was allowed, beginning from the time the drug reached the bath. During this period the stimulus rate was typically 0.1 Hz. A 5 min pause in stimulation followed in order to allow equilibration of inactivation, after which the degree of activity-induced slowing was determined in response to electrical stimulation (usually at 2 Hz) for 180 s. The fibre was then stimulated for a further 10 min at 0.5 Hz, after which a new stimulus trial could begin. Data were collected from only one unit per skull half.

Ion replacement experiments

For sodium replacement experiments all extracellular sodium was replaced with lithium. For experiments in which the concentration of potassium was altered, an equimolar amount of sodium was either added to or removed from the solution. Similarly, reductions in the concentration of extracellular sodium were achieved by equimolar replacement with choline. When EGTA was used to chelate free calcium, 1.5 ml of a 1 M EGTA stock solution was added and the pH of the resulting solution was titrated to 7.4. The 1 M stock solution of EGTA was made up in 0.5 M NaOH to pH 8.0. The additional 0.75 mM sodium resulting from this was not compensated.

Chemicals

Ouabain, sodium cyanide, lidocaine hydrochloride, carbamazepine (CBZ) and phenytoin (5,5-diphenyl-hydantoin) were all obtained from commercial sources (Sigma, Fluka and Calbiochem). All chemicals were diluted to their appropriate concentration in physiological solution on the day of the experiment from pre-prepared stock solutions that ranged in concentration

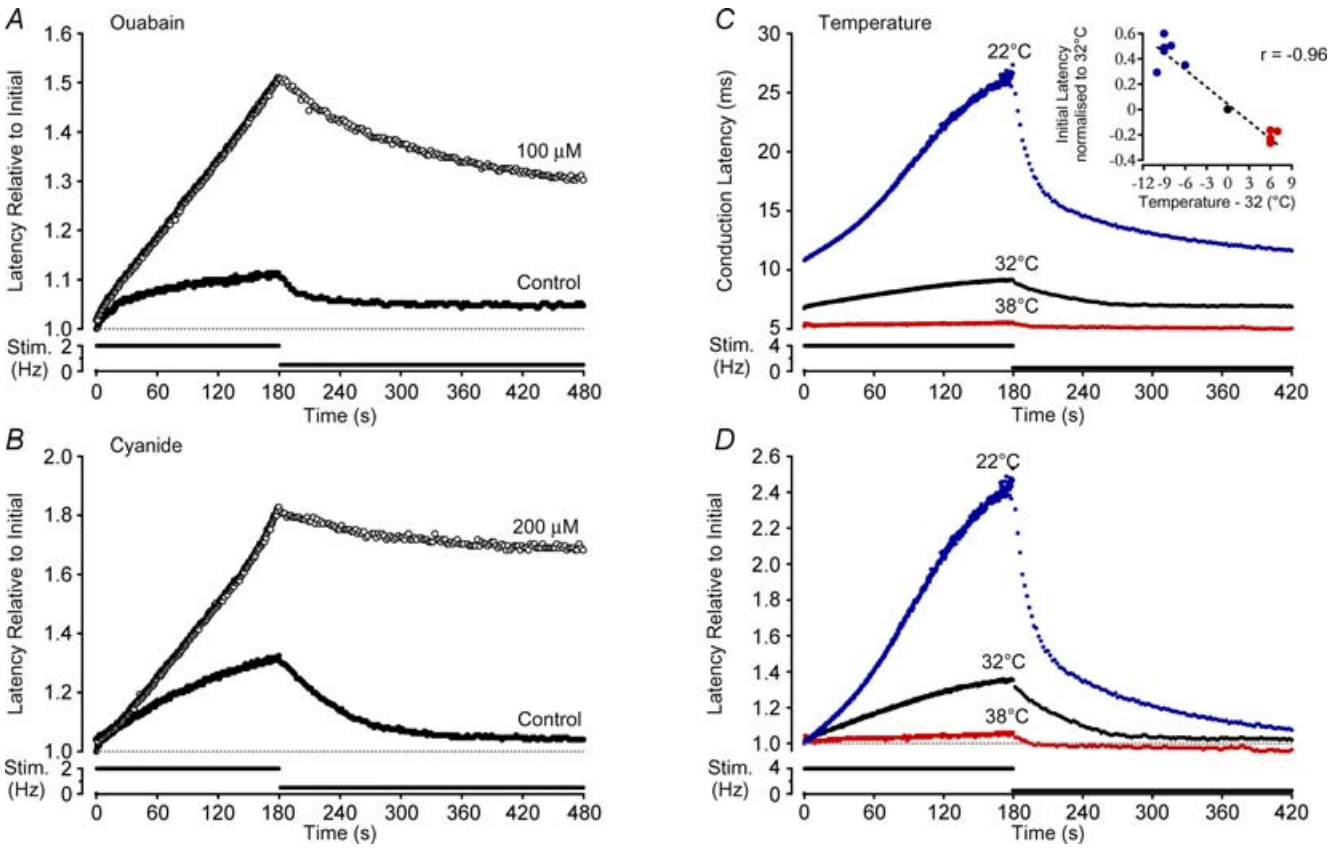

Figure 2. Effect of pharmacological Na^+–K^+-ATPase blockade and temperature on activity-induced changes in conduction velocity
Direct Na^+–K^+-ATPase blockade with ouabain (100 μM, *A*) as well as indirect blockade via disruption of mitochondrial ATP production with cyanide (200 μM, *B*) both result in an increase in conduction velocity changes produced by repetitive stimulation. Increases and decreases in temperature affect the absolute conduction velocity (*C* and inset) as well as the relative change in latency induced by activity (*D*). The effect of temperature alone on activity-induced changes is clear after normalization for the temperature effect on initial latency (*D*).

from 100 mM to 1 M. Stock solutions of ouabain, sodium cyanide, tetrodotoxin (TTX), benzocaine and lidocaine were made up in distilled water while stock solutions of CBZ and phenytoin were made up in DMSO. Control experiments showed that the DMSO vehicle had no effect on activity-induced changes in conduction latency (1.04 ± 0.10-fold change, $n = 4$, data not shown).

Data analysis

All stimulation protocols began after a 300 s period without stimulation. The latency of response to the first stimulus after this pause is referred to here as the initial latency. Conduction latency response profiles to constant frequency electrical stimulation and beginning immediately following the pause were fitted with either a single or double exponential function. The Levenberg–Marquardt algorithm for iterative fitting in Igor Pro was used to determine the fit coefficients. The degree of latency change in response to stimulation, i.e. typically 180 s at 2 Hz, was determined from the value of the fit function at 180 s. Latency measures at 0.5 Hz were determined from the average of values over a 10 s period centred at $t = 480$ s, i.e. 300 s after the transition from a higher to a lower stimulation frequency, typically from 2 Hz to 0.5 Hz.

Average values are quoted as mean and standard error of the mean unless otherwise indicated. Two-way or repeated measures ANOVA or Student's t test were used for statistical comparisons and their use is indicated in the text.

Results

The effect of repetitive activity on axonal conduction velocity, measured as conduction latency, was examined in 70 single axons innervating the rat cranial meninges. The conduction length varied for individual recordings and ranged from 2.8 to 12 mm (mean 6.02 ± 1.8 mm). An example of unitary action potential responses to repeated electrical stimulation is shown in Fig. 1*C*. Conduction velocities of individual axons ranged from 0.10 to 1.43 m s^{-1} (mean 0.55 m s^{-1}, median 0.46 m s^{-1}). Since the intent here was to investigate the process whereby impulse activity modulates conduction velocity, the receptive properties of individual axons were only established if recording conditions permitted this at the end of an experiment. An initial sensory characterization of units was avoided in an attempt to reduce sensitizing effects known to occur, for example, with heat stimulation (Beck *et al.* 1974). For those units tested, 11 of 13 fibres were mechanically sensitive, 3 of 3 were activated by heating and 4 of 4 were sensitive to capsaicin (1 μM). No difference in the time course or the magnitude of activity-induced slowing during 180 s of 2 Hz stimulation was found between those units confirmed as sensory and those for which their designation as sensory was based entirely on their slowing profile.

Characteristics of activity induced changes in conduction latency

For all axons, conduction latency changed in a manner dependent upon the rate of activation and such changes can be characterized by three properties. First, in all axons it is possible to increase the rate of stimulation such that the progressive slowing of conduction velocity eventually gives way to both large jumps in conduction latency and intermittent conduction failures (Figs 1*C*, *D* and 3*C*). The conduction latency at which this occurs for an individual axon we have called the 'critical deficit' latency (see Discussion). When determined at 35.5°C the critical deficit latency occurred on average at 1.92-fold (median 1.94, 1st quartile 1.61, 3rd quartile 2.22, $n = 28$) the initial conduction latency. At stimulation rates that bring the axon to the critical deficit latency the temporal profile of the change in conduction latency was often sigmoidal in form (see Fig. 1*D*). Second, activity-induced changes in conduction latency approach steady state at constant stimulus frequency (see Fig. 1*B*) for all stimulus frequencies below that at which the critical deficit latency is reached. This is shown in Fig. 1*B* by the observation that the same conduction latency is approached from both an initially longer (induced with 2 Hz stimulation) as well as an initially shorter latency (i.e. without preceding stimulation). A nominal single exponential fit yields a time constant for this process of 170 ± 64 s ($n = 7$) when the steady state is approached from a shorter latency and 289 ± 167 s ($n = 3$) when approached from an initially longer latency. Third, the relationship between the rate of activation and steady-state latency is monotonic positive (Fig. 1*E*). In some axons, at low stimulation rates, conduction velocity may actually increase transiently (i.e. speeding) before subsequently slowing to steady state. Interestingly, this speeding behaviour can also be induced by substances that stabilize the inactivated state of sodium channels (see for example Fig. 5).

Role of the Na^+–K^+-ATPase

The increase in intracellular Na^+ that occurs with each action potential increases electrogenic Na^+–K^+-ATPase activity and the axon hyperpolarizes (Rang & Ritchie, 1968; Morita *et al.* 1993). If the voltage threshold for regenerative sodium channel activation is assumed to remain more or less constant, then axonal hyperpolarization increases the amount of charge required to drive regenerative sodium current. Under this premise,

axonal Na^+–K^+-ATPase-mediated hyperpolarization has hitherto been deemed causal for the concomitant reduction in conduction velocity seen with repetitive activity. To test the validity of this assumed causality the effect of Na^+–K^+-ATPase blockade on activity-induced changes in conduction velocity was examined.

Effect of ouabain and cyanide

A significant fraction of the current attributable to Na^+–K^+-ATPase isozymes in small diameter rat DRG neurons is sensitive to the *Strophanthus gratus* plant toxin ouabain (Dobretsov *et al.* 1999*b*). Accordingly, direct pharmacological blockade of the Na^+–K^+-ATPase with ouabain (10^{-4}–10^{-3} M) increased the initial conduction latency by $4.68 \pm 1.47\%$ ($P < 0.05$, paired t test, $n = 10$). Ouabain also increased, by 3.67 ± 1.16-fold, the amount of conduction velocity slowing seen during 180 s stimulation at 2 Hz ($P < 0.05$, paired t test, $n = 10$; Fig. 2*A*). This increase in activity-induced slowing persisted during stimulation at 0.5 Hz and when measured 300 s after the transition from 2 Hz to 0.5 Hz, the conduction latency was 3.55 ± 1.12-fold higher than that at the corresponding time point under control conditions ($P < 0.05$, paired t test, $n = 11$; Fig. 2*A*).

Similar effects to those under ouabain were seen with cyanide (10^{-4}–10^{-3} M), which hampers Na^+–K^+-ATPase activity indirectly by reducing mitochondrial production of ATP. In the presence of cyanide, the initial latency was, on average, not altered. However, the change in conduction latency produced during 180 s stimulation at 2 Hz increased 3.73 ± 1.87-fold ($n = 4$). Similarly, the conduction latency determined 300 s after the transition in stimulation frequency to 0.5 Hz was also increased in the presence of cyanide by an average 11.68 ± 5.84-fold ($n = 4$, Fig. 2*B*).

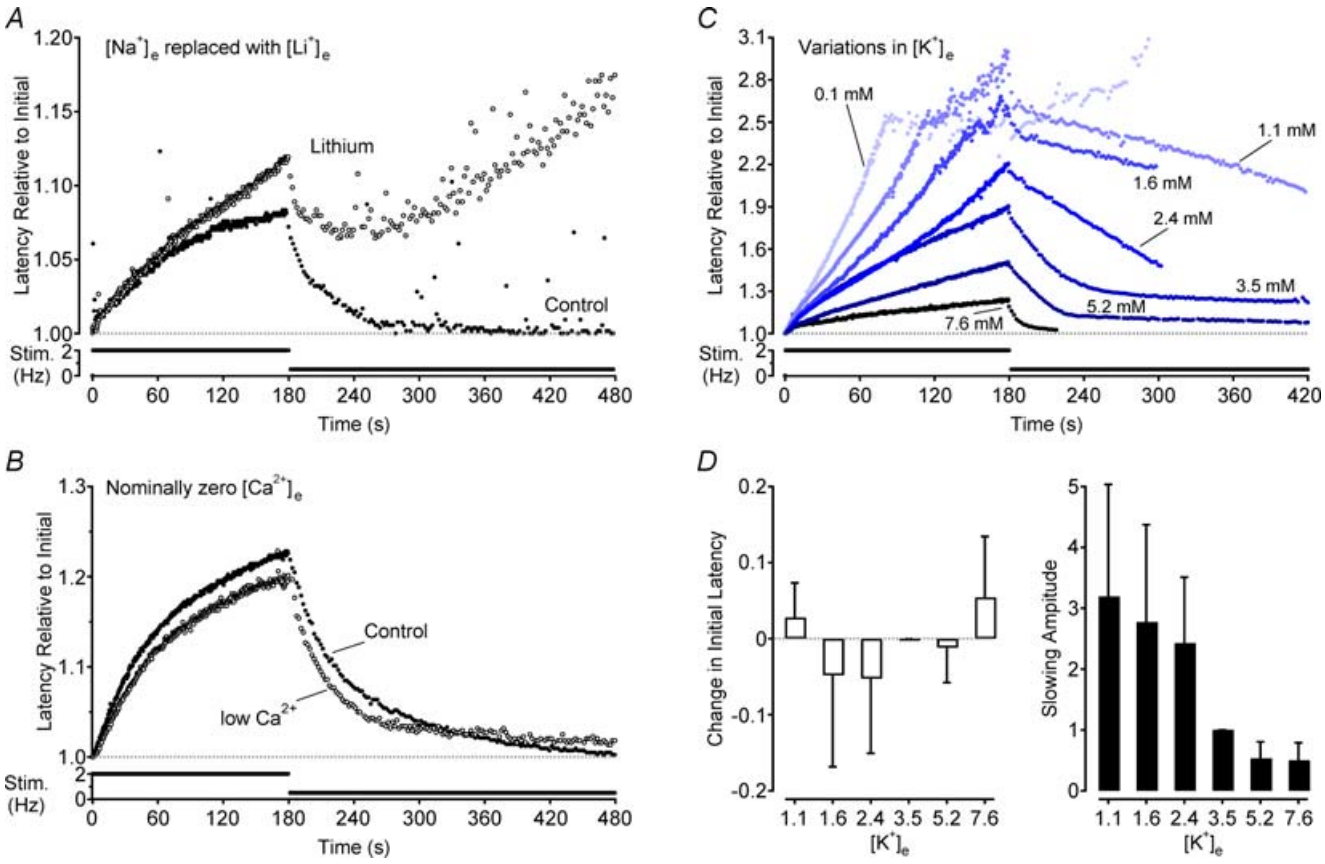

Figure 3. Effects of extracellular ion concentration on activity-induced changes in conduction velocity
Na^+ was completely removed from the extracellular perfusing solution by replacement with an equimolar amount of Li^+ (*A*) and the extracellular concentration of Ca^{2+} was reduced by the addition of 1.5 mM EGTA to the perfusate (*B*). Changes in latency in both cases are shown relative to the initial latency under control conditions. The effect of changes in extracellular K^+ concentration were normalized to the initial latency at that concentration (*C*). Changes in extracellular K^+ were osmotically balanced by removal or addition of an equimolar amount of Na^+. Group means show the effect of each K^+ concentration on both initial latency relative to that for 3.5 mM K^+ and the amplitude of activity-induced slowing (*D*).

Effect of temperature

To further examine the role of Na^+–K^+-ATPase activity in determining axonal conduction velocity, the effect of temperature was examined. As expected, all axons conducted more rapidly at higher temperatures ($r = -0.96$, $P < 0.01$, $n = 11$, Fig. 2*C*, inset). To determine the effect of temperature on activity-induced changes in latency, conduction latency measures were normalized to the initial latency at each temperature (Fig. 2*D*). Na^+–K^+-ATPase activity is positively correlated with temperature (Senft, 1967) and therefore, if the hyperpolarizing effect of increased Na^+–K^+-ATPase activity were causal for activity-induced increases in conduction latency, it would be expected that the magnitude of latency changes during stimulation would be reduced by cooling and increased by warming.

When tested, precisely the opposite was found. Cooling increased, while warming decreased the amount of conduction velocity slowing in response to 180 s of 2 Hz electrical stimulation ($P < 0.01$, ANOVA, d.f. = 17, Fig. 2*D*). As with ouabain and cyanide, temperature also influenced the rate of recovery of conduction latency upon transition to a lower frequency of activation. At 32°C the time constant of recovery over the 300 s following the transition from high to low frequency stimulation was on average 35.95 ± 14.68 s. When the preparation was cooled by an average 8.5 ± 1.38°C the rate of recovery of conduction latency over the same period was 115.55 ± 49.88 s, and when the preparation was warmed by 6.2 ± 0.4°C, this value fell to 26.30 ± 9.08 s ($P < 0.01$, ANOVA, d.f. = 17; Fig. 2*D*).

Effect of replacing extracellular sodium with lithium

Since temperature affects a range of physico-chemical processes the role of Na^+–K^+-ATPase activity was also examined under conditions of reduced ionic substrate. In the first instance, extracellular Na^+ was replaced with lithium (Li^+). Lithium's ability to permeate sodium channels is very close to that for Na^+ (i.e. $P_{Li}/P_{Na} \approx 0.93$, Hille, 1971) but Li^+ is poorly extruded by the Na^+–K^+-ATPase (Thomas, 1972). In the absence of impulse activity, the replacement of extracellular Na^+ with Li^+ did not affect the initial latency. During 2 Hz stimulation, however, the latency response profile in the presence of Li^+ deviates away from that of the control profile and in the example record of Fig. 3*A* this occurs after approximately 130 pulses. A progressive enhancement in the amount of latency increase with each subsequent stimulus is apparent as stimulation continues beyond this point, such that after 180 s of 2 Hz stimulation the latency was on average 1.32 ± 0.49-fold ($P < 0.01$, paired *t* test, $n = 7$) that observed during the control period (Fig. 3*A*). Since intracellular Na^+ is not replenished, Na^+–K^+-ATPase activity continues to decline with each subsequent action potential and there is little recovery of latency even after the transition from 2 to 0.5 Hz, and 300 s subsequent to this transition the latency is on average 7.81 ± 3.91-fold larger ($P < 0.05$, paired *t* test, $n = 7$) in the presence of Li^+ (Fig. 3*A*).

Effect of varying extracellular potassium concentration

The extracellular K^+ concentration is rate limiting for Na^+–K^+-ATPase activity and therefore the effect of systematically varying extracellular K^+ concentration on activity-induced changes in conduction latency was also examined. In the absence of activity, changes in the Nernst potential for K^+ are expected to dominate. If membrane potential itself were to affect conduction velocity, then depolarization should speed conduction and hyperpolarization should slow conduction. Such an effect should be reflected in changes in the initial latency of conduction measured after a 300 s pause in stimulation. In contrast to this expectation, changes in extracellular K^+ concentration did not significantly change the initial conduction latency (Fig. 3*D*). If anything, small deviations from 3.5 mM extracellular K^+ tended to speed conduction velocity while larger excursions in extracellular K^+ slowed conduction velocity.

During repetitive stimulation, axonal membrane potential will be affected by the rate of electrogenic Na^+–K^+-ATPase extrusion of intracellular Na^+. Under conditions of low extracellular K^+, Na^+–K^+-ATPase activity is compromised allowing intracellular Na^+ to accumulate with each action potential. The depolarizing effect of this accumulation is likely to be compensated to some extent by an outward movement of K^+. However, owing to the rather limited intracellular volume of thin unmyelinated axons, the outward K^+ current may abate quite rapidly with the net result being depolarization of the axon. Applying this rationale, if membrane potential were the primary determinant of conduction velocity then under conditions of low extracellular K^+ a reduction in activity-induced slowing, or even a speeding, might be expected. Conversely, when extracellular K^+ is increased, the Na^+–K^+-ATPase can extrude the intracellular Na^+ load accompanying each action potential more promptly and the axon would be expected to hyperpolarize more strongly, resulting in a more pronounced conduction latency increase. As shown in Fig. 3*C*, the opposite effect is observed, namely decreases in extracellular K^+ concentration increase the amount of activity-induced conduction velocity slowing while elevation of the extracellular K^+ concentration decreases the amount of activity-induced conduction velocity slowing ($P < 0.01$, ANOVA, d.f. = (6,22); Fig. 3*C* and *D*.

The effects of pharmacological blockade of the Na^+–K^+-ATPase, temperature, extracellular replacement of Na^+ with Li^+ and the effects of varied extracellular K^+ all demonstrate that Na^+–K^+-ATPase-mediated hyperpolarization is not causal for activity-induced conduction velocity slowing. Instead quite the opposite is the case, namely increased Na^+–K^+-ATPase activity acts to prevent or at least limit conduction velocity slowing. This is further confirmed by the striking correlation between extracellular K^+ concentration and the rate of conduction latency decrease upon decreasing stimulation frequency (Fig. 3*C*). Low extracellular K^+, for which Na^+–K^+-ATPase efficacy is compromised, prolonged the rate of conduction velocity recovery upon transition to a lower stimulus frequency while high extracellular K^+ concentrations speed the rate of recovery (see Fig. 3*C*).

Effect of reduced extracellular calcium

Repetitive action potential activity leads to an increase in the intra-axonal calcium concentration (Gover *et al.* 2003) and potentially to the activation of Ca^{2+}-activated potassium channels (Jirounek *et al.* 1991). Activation of Ca^{2+}-activated potassium channels may produce a slowing of axonal conduction velocity via both their hyperpolarizing effect and their contributing to a reduction of net membrane resistance. Consequently, the influence of changes in extracellular Ca^{2+} on activity-induced conduction velocity slowing was examined. The concentration of extracellular Ca^{2+} was reduced by adding 1.5 mM EGTA to the perfusing solution. This had no effect on the initial latency after a 300 s pause and was also without appreciable effect on activity-induced changes in conduction latency ($n = 4$, final free $[Ca^{2+}]_o$ ~0.5 mM, Fig. 3*B*).

Effect of reduced extracellular sodium

It could be argued that the changes observed in the presence of Na^+–K^+-ATPase modulation were secondary to changes in intracellular Na^+ (see Discussion). To examine this possibility the effect of a reduction in the extracellular Na^+ concentration was examined. Reduction of the extracellular Na^+ concentration by 20 and 50 mM, through replacement with an equimolar amount of choline, produced respective increases in the initial latency of $4.10 \pm 2.36\%$ ($n = 3$) and $11.89 \pm 5.94\%$ ($n = 4$, Fig. 4*A*). The degree of conduction latency change produced with repetitive activity was more pronounced under conditions of low extracellular Na^+, at both 2 Hz (1.28 ± 0.74-fold at 20 mM and 1.39 ± 0.69-fold at 50 mM, $n = 3$) and after a subsequent 300 s period of stimulation at 0.5 Hz (5.33 ± 3.08-fold at 20 mM and 7.17 ± 3.59-fold at 50 mM, $n = 4$, Fig. 4*A*).

The role of sodium channel availability in conduction velocity modulation

The evidence presented above demonstrates that during constant frequency stimulation Na^+–K^+-ATPase-mediated hyperpolarization is not causally coupled to a slowing in axonal conduction velocity. Indeed, Na^+–K^+-ATPase activity actually limits the extent of activity-induced conduction velocity slowing. To explain this we propose that it is primarily the modulation of sodium channel availability that regulates axonal conduction velocity and evidence in support of this proposal follows.

Effects of TTX

Tetrodotoxin (TTX) binds to and blocks sodium channel α-subunits and thereby reduces the absolute number of TTX-Sensitive (TTXs) sodium channels available for conduction. Accordingly, TTX (10–30 nM) increased dose-dependently the initial latency (1.146 ± 0.04-fold, $P < 0.01$, paired t test, $n = 11$) and, at sufficient dose, eventually blocked axonal conduction (Fig. 4*B*). TTX binds specifically to sodium channels and therefore, for subblocking doses, the effect of TTX during repetitive activity should be chiefly to reduce the absolute amount of Na^+ entry during each action potential. Consistent with this, TTX increased the degree of conduction velocity slowing seen in response to stimulation at 2 Hz (1.41 ± 0.44-fold, $P < 0.01$, paired t test, $n = 11$). This is apparent in Fig. 4*B*, where 10 nm TTX produces practically no change in the initial latency, yet a small increase in the slowing effect of repetitive activity. For progressively increasing doses of TTX (20–60 nM) the profile of activity-induced changes in latency remains similar to that at 10 nM TTX, and this profile sums with the dose-dependent increases in initial latency produced with TTX. For this fibre, 60 nM TTX is marginally below that required for conduction block (cf. conduction block at 70 nM, grey markers), yet changes in conduction velocity persist during activity at 2 Hz. For the six units examined, the latency at which TTX produced conduction block was always below the critical deficit latency, i.e. the latency at which activity itself produced conduction block (data not shown).

Effect of lidocaine and carbabmazepine

The local anaesthetic lidocaine and the anti-convulsant carbamazepine (CBZ) both exert a tonic block of sodium channels by binding to and stabilizing the inactivated states of the channel. For single unmyelinated axons this effect is reflected in a dose-dependent increase in initial latency for both lidocaine (10–300 μM; $P < 0.01$, ANOVA, d.f. = 3,7; Fig. 5*C*) and CBZ (30–500 μM; $P < 0.01$, ANOVA, d.f. = 3,12; Fig. 5*F*). The increase in

initial latency produced by both substances summed non-linearly and eventually masked activity-induced changes in latency. At low doses (~30 μM for lidocaine and < 100 μM for CBZ) the increase in initial latency is accompanied by an enhancement of activity-induced changes in latency (Fig. 5*A*, *D*). At higher doses, activity-induced changes in conduction latency are progressively reduced in magnitude. Indeed, at sufficiently high doses, activity-induced changes in conduction latency were essentially abolished (e.g. Fig. 5*B*, lidocaine 100 μM; Fig. 5*E*, CBZ 300 μM). Importantly, this apparent block of activity-induced slowing was dependent upon the frequency of stimulation, such that an increase in stimulus rate produced a demonstrable increase in conduction latency (grey traces, Fig. 5*B* and *E*).

Of interest, an initial reduction of conduction latency was observed (see Fig. 5*E*, CBZ, 700 μM) for moderate doses of lidocaine (>100 μM) and CBZ (>500 μM). This initial speeding of conduction velocity was observed in all fibres tested with lidocaine and CBZ although the extent of this phenomenon varied between individual axons (Fig. 5*A* and *C*). Similar effects to that described for lidocaine and CBZ were also observed for phenytoin (100–500 μM, $n = 3$, data not shown). Additionally,

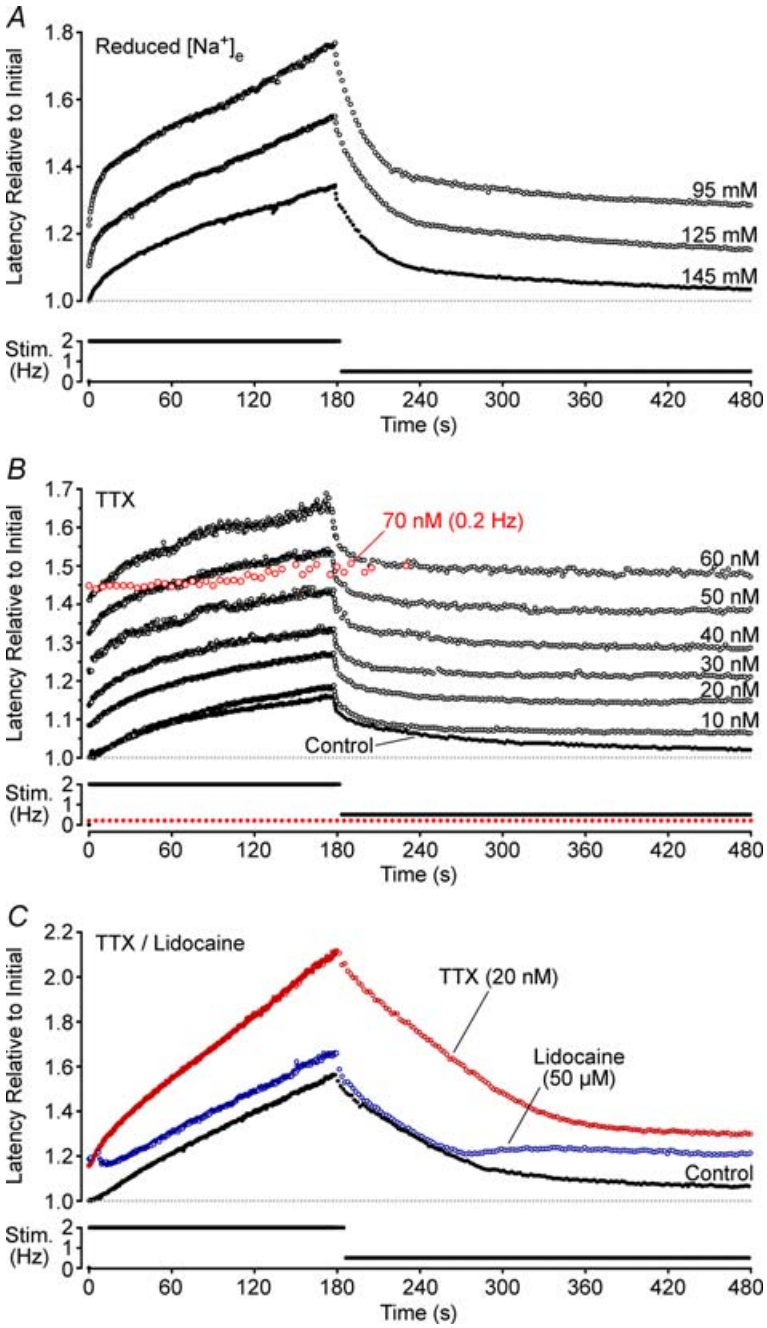

Figure 4. Effects of reduced extracellular Na^+ and the sodium channel blockers TTX and lidocaine on activity-induced changes in conduction latency
Data from four individual axons is shown, respectively, in each panel. Extracellular Na^+ concentration was reduced by replacement with an equimolar amount of choline (*A*). *B* shows the effect of increasing doses of TTX on activity-induced slowing (10–70 nM), as well as the block of conduction by TTX at 70 nM (open grey symbols). In this example, TTX blocks conduction at 70 nM while at 60 nM changes in conduction latency produced by activity exceed the TTXs latency. In *C*, TTX (20 nM) and lidocaine (50 μM) produced a similar shift in base latency for this axon allowing a direct comparison of the effects of the two substances. Changes in latency are shown relative to the initial latency under control conditions.

an oscillation in conduction velocity is seen upon transition from high to lower stimulus frequency for lidocaine (Fig. 5*A*) and sometimes in the presences of CBZ and phenytoin but not for benzocaine.

Discussion

The proposal that Na^+–K^+-ATPase-driven hyperpolarization is causal for the slowing of conduction velocity that accompanies repetitive activity was examined in single unmyelinated axons innervating the rat cranial dura. In contrast to expectation, Na^+–K^+-ATPase blockade results in an enhanced activity-induced conduction velocity slowing, while manipulations expected to increase Na^+–K^+-ATPase activity reduce the extent of slowing. To reconcile this we propose that axonal conduction velocity is modulated primarily by changes in available sodium channel number. Specifically, the slowing of conduction velocity that occurs following a preceding action potential reflects that proportion of sodium channels still in their slow inactivated state. Changes in membrane potential that accompany impulse activity, such as the well-described Na^+–K^+-ATPase-mediated hyperpolarization, can also modulate conduction velocity but do so secondarily by altering the average rate of sodium channel state transition. This coupling is able to account for both the enhancement of activity-induced conduction velocity slowing during Na^+–K^+-ATPase

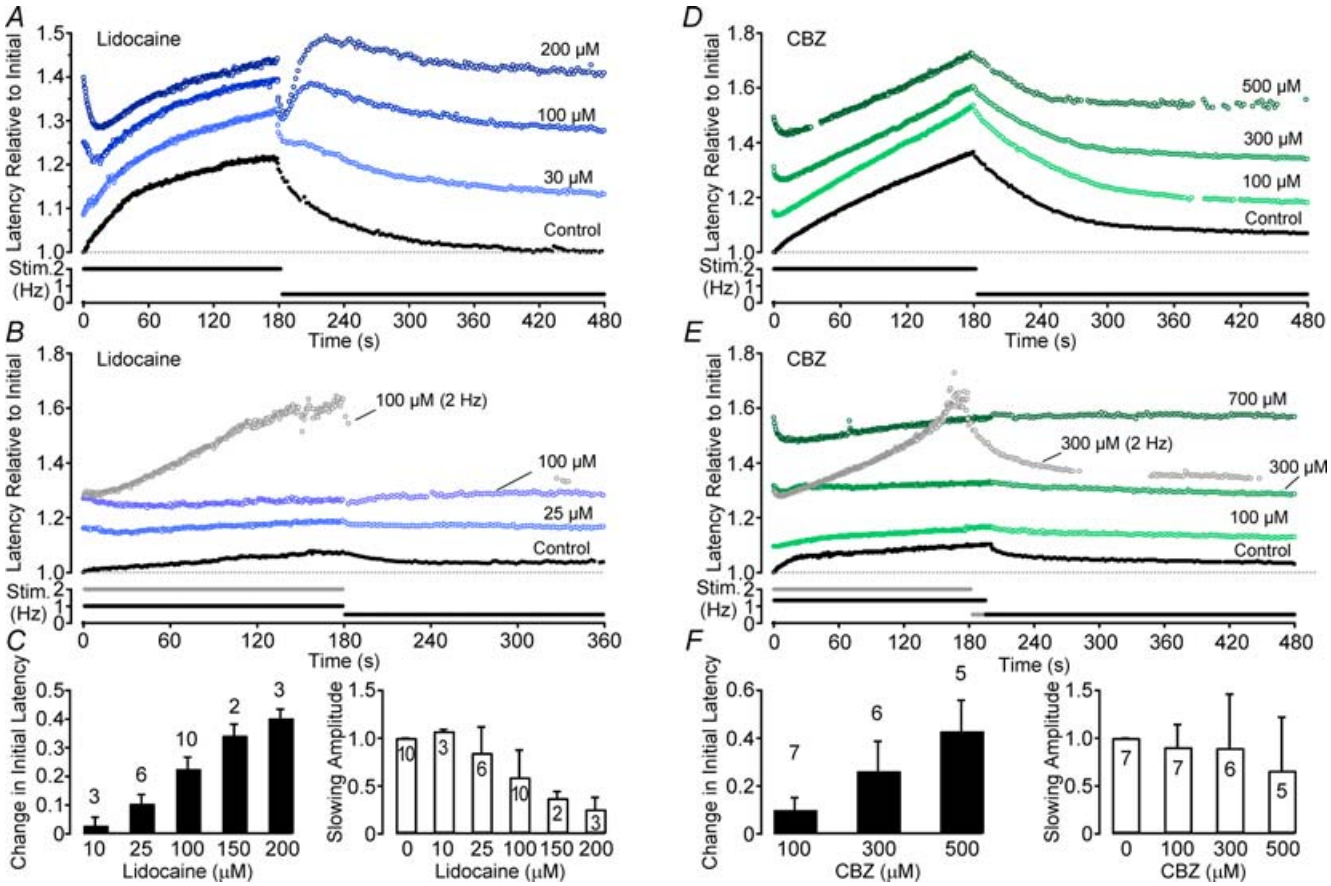

Figure 5. Effects of the anti-convulsant carbamazepine (CBZ) and the local anaesthetic lidocaine on activity-induced changes in conduction latency
Different doses of CBZ and lidocaine were added to the solution and the electrical stimulation protocol was carried out at each dose. For both compounds low doses result in an increase in the amplitude of slowing during a 180 s period of stimulation at 2 Hz (*A* and *D*). As the dose increases an initial speeding of conduction latency becomes apparent. For lower frequencies of stimulation it is possible to increase the dose of both lidocaine and CBZ so that no slowing of conduction latency is observed in response to electrical stimulation (*B* and *E*). However, if the stimulation frequency is increased, it is still possible to induce activity-induced conduction velocity slowing as shown for one trial in 300 μM CBZ (*E*) and one trial in 100 μM lidocaine (*B*). Both the stimulation profile and the response to this higher rate of stimulation are shown in grey. Group data for lidocaine (*C*) and CBZ (*F*) are shown according to the dose-dependent effect on the initial latency (filled bars) and the amplitude of activity-induced slowing (open bars). Changes in latency are shown relative to the initial latency under control conditions.

blockade as well as its curtailment by substances that stabilize the inactivated state of sodium channels.

The possibility that sodium channel availability could be the primary determinant of relative changes in the conduction velocity of unmyelinated sensory axons during activity was first suggested by Bliss & Rosenberg (1979) who subsequently dismissed the idea and opted for an accumulation of intracellular Na^+ as the responsible mechanism. A progressive reduction in the Nernst potential for Na^+ during repetitive activity could account for both conduction velocity slowing and its enhancement by Na^+–K^+-ATPase blockade (Figs 2 and 3) as slowed conduction velocity resulting from a reduction in the Nernst potential for Na^+ is well established (Hodgkin & Katz, 1949 and see also Fig. 4*A*). For manipulations such as TTX application and low dose lidocaine and CBZ, the absolute amount of Na^+ entering the axon per pulse would be expected to be reduced and thereby presumably also the rate of intracellular Na^+ accumulation. However, all of these manipulations increase the magnitude of conduction velocity slowing (Figs 4 and 5). Similarly, in the dendrites of hippocampal CA1 pyramidal neurons, activity-induced reductions in action potential amplitude are enhanced by the application of TTX (100 nM) (Colbert *et al.* 1997). Figure 4 demonstrates that a reduction in extracellular Na^+ and with it presumably a reduced rate of intracellular Na^+ accumulation also results in an enhancement of activity-induced slowing. The interpretation of this result is confounded, however, by the higher likelihood of entry into slow inactivation for sodium channels when extracellular Na^+ is replaced with impermeant organic cations (Townsend & Horn, 1997). Nevertheless, the enhancement of activity-induced slowing under conditions of reduced Na^+ entry during the action potential, is interpreted here as resulting from a reduction in Na^+–K^+-ATPase-mediated hyperpolarization and thereby a reduced retrieval of sodium channels from activity-induced inactivation. Therefore, while changes in the Nernst potential for Na^+ most certainly affect conduction velocity, the influence of this during repetitive activity is considered to be small relative to the effect of cumulative slow inactivation of sodium channels.

Activity-induced changes in sodium channel availability

In small diameter DRG neurons with unmyelinated axons, $Na_V1.8$ (Akopian *et al.* 1996) and $Na_V1.9$ (Dib-Hajj *et al.* 1998) are the predominant TTX-resistant (TTXr) sodium channels expressed. TTXr current contributes substantially during the action potential in both the cell soma (Blair & Bean, 2002) and the nerve terminal (Carr *et al.* 2002). Reductions in the magnitude of both TTXs and TTXr current, attributable to slow inactivation, can be induced by either prolonged depolarization (Ogata & Tatebayashi, 1992) or repetitive depolarizing pulses of medium duration (Roy & Narahashi, 1992; Rush *et al.* 1998; Fazan *et al.* 2001; Tripathi *et al.* 2006) and, in particular for TTXr current, in response to repetitive action potential voltage profiles (Blair & Bean, 2003). Activity-induced reductions in sodium channel availability have also been demonstrated in the dendrites of hippocampal CA1 pyramidal neurons (Colbert *et al.* 1997; Mickus *et al.* 1999) where, as a result, both a reduction in the amplitude of the back-propagating action potential as well as a reduction in its efficacy of conduction ensues (Jung *et al.* 1997). Although not explicitly reported in dendrites, a reduction in available sodium channel number brought about by impulse activity would also be expected to slow the speed of impulse conduction.

Accordingly, an activity-dependent reduction in sodium channel availability is considered to provide an adequate explanation for all three features of conduction velocity slowing seen in unmyelinated peripheral axons (see Fig. 1). Firstly, the symmetry and very long time course of conduction velocity changes observed in response to constant frequency stimulation (*ca* 800–900 s; see Fig. 1*D*) are comparable with the time course of TTXr current inactivation in rat DRGs under voltage clamp, for which steady state is achieved after about 800 s for both depolarizing and hyperpolarizing voltage steps (Ogata & Tatebayashi, 1992). An alternative explanation for time courses of this magnitude via Na^+–K^+-ATPase-mediated hyperpolarization or intracellular Na^+ clearance is difficult to reconcile. Secondly, the relationship between impulse frequency and steady-state conduction latency for an individual axon is monotonic positive. The proposal is that the steady-state conduction latency achieved at constant frequency stimulation reflects an equilibrium between the number of sodium channels entering inactivation during each impulse and the average time spent in this state, which is determined by membrane potential; the rate of retrieval being prolonged by depolarization and shortened by hyperpolarization (Rush *et al.* 1998; Ogata & Tatebayashi, 1992). As stimulus frequency increases, recruitment of inactivated sodium channels would be expected to increase proportionally more than Na^+–K^+-ATPase activity, shifting the point of equilibrium towards longer steady-state conduction latencies (see Fig. 1*E*). Support for this can be taken from manipulations that alter the coupling between these two processes, for example Na^+–K^+-ATPase blockade or reductions in the absolute Na^+ entry per action potential, which result in a more pronounced slowing of axonal conduction in response to repetitive stimulation (see Figs 2–4).

Cumulative sodium channel inactivation also provides an adequate explanation for the critical deficit latency (see Fig. 1*C* and *D*), that is, the latency at which an individual fibre begins to exhibit intermittent conduction

failures and simultaneously large jumps in conduction latency (see also Fig. 3*C*). The critical deficit latency is interpreted as corresponding to the point at which activity-induced reductions in sodium channel availability along the axon have progressed to such an extent that some segments of axon are no longer able to support regenerative conduction. The number and spatial extent of such regions determines the size of the variations in conduction latency. Conduction failures correspond to contiguous regions of axon over which the electrotonic decrement in voltage is sufficient to abrogate regenerative conduction in the proximal axon. Consistent with this model, conduction failures have been reported at high rates of stimulation in dendrites (Spruston *et al.* 1995) and have also been observed in unmyelinated sensory afferents in humans (Weidner *et al.* 2003).

Interaction of pharmacologically induced and activity-induced inactivation

Lidocaine and CBZ bind preferentially to open and inactivated states of sodium channels and stabilize the latter (Sandtner *et al.* 2004; Cardenas *et al.* 2006). As a higher percentage of TTXs channels are inactivated at potentials near rest, both substances exert more tonic block of TTXs current than TTXr (Leffler *et al.* 2007). Accordingly, at low doses of lidocaine and CBZ a shift in initial latency is observed, the magnitude of activity-induced slowing is slightly increased and these two effects sum (Fig. 5*A* and *D*), an effect similar to that seen with TTX (Fig. 4*B*). The interpretation is that a reduction in TTXs channel number slows conduction speed accounting for the shift in initial latency and also reduces Na^+ entry during the action potential, leading to an enhanced activity-induced slowing resulting from the uncoupling of Na^+–K^+-ATPase activity and inactivation. Further increases in dose progressively increase the initial latency and reduce the amplitude of activity-induced slowing and eventually the shift in initial conduction latency completely occludes the activity-induced changes in latency (Fig. 5*B* and *E*). Native TTXr currents that display the most prominent use-dependence are those most sensitive to block by phenytoin and CBZ (Rush & Elliott, 1997). The dose-dependent pharmacological block of TTXr therefore parallels the proposed frequency-dependent inactivation of TTXr. For a given frequency of stimulation, pharmacological substances that reduce TTXr current via stabilized inactivation would therefore be expected to reduce the absolute magnitude of activity-induced changes in velocity and, as observed at higher doses, eventually occlude activity-induced changes in conduction velocity completely. That is, those channels that would otherwise be inactivated at a given stimulus frequency are already pharmacologically stabilized in inactivation.

TTXr contributes to changes in membrane potential during the action potential, with the magnitude of the current being most probably larger than the TTXs portion (Blair & Bean, 2002; Carr *et al.* 2002; Renganathan *et al.* 2001). However, the absolute amount of $Na_V1.8$ protein in the cell soma is not correlated with conduction velocity of the central projecting axon (Djouhri *et al.* 2003) while $Na_V1.9$ content and conduction velocity are negatively correlated (Fang *et al.* 2002). In general, cell determined current kinetics cannot be simply interpreted in terms of axonal action potential conduction particularly where neither the relative spatial distribution nor the relative density of sodium channel subtypes are known. It is nonetheless reasonable to speculate that axonal conduction in unmyelinated afferents relies sufficiently heavily upon total TTXr current that a change in its magnitude and/or kinetics can affect conduction velocity.

Interestingly, an initial speeding of conduction velocity was seen in response to repetitive stimulation in the presence of lidocaine and CBZ but not TTX (see Fig. 5*A* and *D*). The speeding became more pronounced with increasing dose. An initial speeding of conduction velocity is also seen under control conditions in some human C-fibres in response to low frequency stimulation. Gokin *et al.* (2001) observed a similar phenomenon in the form of recovery from lidocaine-induced axonal conduction block during repetitive stimulation. They interpreted this as a relief of tonic block via Na^+–K^+-ATPase-mediated hyperpolarization. Presently, however, we cannot offer a satisfactory explanation for the initial reduction in conduction velocity seen in the presence of lidocaine and CBZ. A second point of interest is the oscillation in conduction velocity observed upon transition from high to low frequency stimulation in the presence of lidocaine (Fig. 5*A*). This feature appears to be associated with local anaesthetic use-dependence, being prominent for lidocaine but absent in the presence of benzocaine, which shows minimal use-dependence in its action on Na^+ channels (data not shown).

In response to repetitive depolarizing pulses, TTXr current in DRG neurons shows a more pronounced inactivation than TTXs current (Rush *et al.* 1998). Similarly, when repetitively activated with short-duration depolarizing pulses at 1–2 Hz, cell expressed $Na_V1.8$ showed substantially more inactivation than $Na_V1.7$ (Vijayaragavan *et al.* 2004). The suggestion is then that the subtype of channels that progressively accumulate in their inactivated state during repetitive activity is frequency dependent, i.e. as the frequency increases TTXr and subsequently TTXs channels are reduced in number. Previous reports have suggested that activity-induced slowing occurs predominantly in the distal most portion of axons (Weidner *et al.* 2000; Bostock *et al.* 2003). In accordance with this, TTXr current density is sufficient to support regenerative conduction in nerve terminals (Brock

et al. 1998; Carr *et al.* 2002). By extension, this implies that changes in conduction velocity brought about by changes in TTXr current density may well be expected to parallel changes in excitability.

In the experiments reported here, complete conduction block by TTX required doses ranging from 8 to 80 nM. The lower end of this range is consistent with the IC_{50} values of TTXs sodium channel subtypes (Catterall *et al.* 2005). The upper end of this range, however, may well be influenced by drug access to the axolemma. Nevertheless, 80 nM TTX is not beyond the concentration required for complete block of native TTXs currents in DRG somata (Elliott & Elliott, 1993) and is also below doses of TTX (100 nM) that do not block dendritic conduction in slice preparations (Colbert *et al.* 1997). In general, however, this raises the question as to what magnitude of TTXs current is actually required for conduction in axons co-expressing TTXr currents. Indeed, in axons expressing multiple sodium channel subtypes, conduction is perhaps only enabled through a functional interplay of channel subtypes.

The profile of activity-induced changes in conduction velocity correlate to some degree with the receptive properties of axons (Raymond *et al.* 1990; Thalhammer *et al.* 1994; Gee *et al.* 1996) and these are likely to arise, at least in part, from heterogeneities in the expression of Na^+–K^+-ATPase isozymes (Dobretsov *et al.* 1999*a*,*b*) as well as sodium channel subtypes (see Wood *et al.* 2004 for review). Of particular interest is the apparently insensitive subpopulation of human cutaneous afferents, some of which become sensitive to sensory stimuli subsequent to application of mustard oil or capsaicin (Schmidt *et al.* 1995). Mechanically insensitive afferents display pronounced conduction velocity slowing, have comparatively high electrical activation thresholds and low conduction velocities (Serra *et al.* 1999; Weidner *et al.* 1999). All of these features would be consistent with a reduced basal availability of sodium channels and suggests that a higher threshold for the transformation of generator current into action potential discharge contributes to the 'silence' of this subpopulation of nociceptors.

A further point that remains to be clarified is to determine the extent to which activity-induced sodium channel inactivation affects conduction in the period immediately following an action potential (*ca* 300 ms), a period during which changes in membrane potential are thought to causally modulate conduction velocity (Barrett & Barrett, 1982; Weidner *et al.* 2000; Bostock *et al.* 2003; George *et al.* 2007).

Conclusion

For moderate discharge rates, the conduction speed of unmyelinated somatic axons is determined by the dynamic equilibrium between the slowing effect of cumulative sodium channel inactivation and the speeding effect of Na^+–K^+-ATPase-mediated hyperpolarization. By extension, changes in conduction velocity should therefore reflect, at least partially, changes in excitability, i.e. long-term depolarization would be expected to suppress excitability while hyperpolarization should enhance it. This, of course, does not mean that changes in excitability result exclusively from changes in sodium channel availability. The long-term regulation of axonal conduction velocity through, largely TTXr, sodium channel availability further extends the already prominent role of TTXr channels in spike frequency adaptation (Blair & Bean, 2003) and action potential initiation (Brock *et al.* 1998) in neurons with unmyelinated axons.

References

Akopian AN, Sivilotti L & Wood JN (1996). A tetrodotoxin-resistant voltage-gated sodium channel expressed by sensory neurons. *Nature* **379**, 257–262.

Andres KH, von During M, Muszynski K & Schmidt RF (1987). Nerve fibres and their terminals of the dura mater encephali of the rat. *Anat Embryol (Berl)* **175**, 289–301.

Barrett EF & Barrett JN (1982). Intracellular recording from vertebrate myelinated axons: mechanism of the depolarizing afterpotential. *J Physiol* **323**, 117–144.

Beck PW, Handwerker HO & Zimmermann M (1974). Nervous outflow from the cat's foot during noxious radiant heat stimulation. *Brain Res* **67**, 373–386.

Blair NT & Bean BP (2002). Roles of tetrodotoxin (TTX) -sensitive Na^+ current, TTX-resistant Na^+ current, and Ca^{2+} current in the action potentials of nociceptive sensory neurons. *J Neurosci* **22**, 10277–10290.

Blair NT & Bean BP (2003). Role of tetrodotoxin-resistant Na^+ current slow inactivation in adaptation of action potential firing in small-diameter dorsal root ganglion neurons. *J Neurosci* **23**, 10338–10350.

Bliss TV & Rosenberg ME (1979). Activity-dependent changes in conduction velocity in the olfactory nerve of the tortoise. *Pflugers Arch* **381**, 209–216.

Bostock H, Campero M, Serra J & Ochoa J (2003). Velocity recovery cycles of C fibres innervating human skin. *J Physiol* **553**, 649–663.

Brock JA, McLachlan EM & Belmonte C (1998). Tetrodotoxin-resistant impulses in single nociceptor nerve terminals in guinea-pig cornea. *J Physiol* **512**, 211–217.

Campero M, Serra J, Bostock H & Ochoa JL (2004). Partial reversal of conduction slowing during repetitive stimulation of single sympathetic efferents in human skin. *Acta Physiol Scand* **182**, 305–311.

Cardenas CA, Cardenas CG, de Armendi AJ & Scroggs RS (2006). Carbamazepine interacts with a slow inactivation state of NaV1.8-like sodium channels. *Neurosci Lett* **408**, 129–134.

Carr RW, Pianova S & Brock JA (2002). The effects of polarizing current on nerve terminal impulses recorded from polymodal and cold receptors in the guinea-pig cornea. *J Gen Physiol* **120**, 395–405.

Catterall WA, Goldin AL & Waxman SG (2005). International Union of Pharmacology. XLVII. Nomenclature and structure-function relationships of voltage-gated sodium channels. *Pharmacol Rev* **57**, 397–409.

Colbert CM, Magee JC, Hoffman DA & Johnston D (1997). Slow recovery from inactivation of Na^+ channels underlies the activity-dependent attenuation of dendritic action potentials in hippocampal CA1 pyramidal neurons. *J Neurosci* **17**, 6512–6521.

Dib-Hajj SD, Tyrrell L, Black JA & Waxman SG (1998). NaN, a novel voltage-gated Na channel, is expressed preferentially in peripheral sensory neurons and down-regulated after axotomy. *Proc Natl Acad Sci U S A* **95**, 8963–8968.

Djouhri L, Fang X, Okuse K, Wood JN, Berry CM & Lawson SN (2003). The TTX-resistant sodium channel Nav1.8 (SNS/PN3): expression and correlation with membrane properties in rat nociceptive primary afferent neurons. *J Physiol* **550**, 739–752.

Djouhri L & Lawson SN (2001). Increased conduction velocity of nociceptive primary afferent neurons during unilateral hindlimb inflammation in the anaesthetised guinea-pig. *Neuroscience* **102**, 669–679.

Dobretsov M, Hastings SL & Stimers JR (1999*a*). Non-uniform expression of α subunit isoforms of the Na^+/K^+ pump in rat dorsal root ganglia neurons. *Brain Res* **821**, 212–217.

Dobretsov M, Hastings SL & Stimers JR (1999*b*). Functional Na^+/K^+ pump in rat dorsal root ganglia neurons. *Neuroscience* **93**, 723–729.

Elliott AA & Elliott JR (1993). Characterization of TTX-sensitive and TTX-resistant sodium currents in small cells from adult rat dorsal root ganglia. *J Physiol* **463**, 39–56.

Fang X, Djouhri L, Black JA, Dib-Hajj SD, Waxman SG & Lawson SN (2002). The presence and role of the tetrodotoxin-resistant sodium channel $Na_v1.9$ (NaN) in nociceptive primary afferent neurons. *J Neurosci* **22**, 7425–7433.

Fazan R Jr, Whiteis CA, Chapleau MW, Abboud FM & Bielefeldt K (2001). Slow inactivation of sodium currents in the rat nodose neurons. *Auton Neurosci* **87**, 209–216.

Gee MD, Lynn B & Cotsell B (1996). Activity-dependent slowing of conduction velocity provides a method for identifying different functional classes of C-fibre in the rat saphenous nerve. *Neuroscience* **73**, 667–675.

George A, Serra J, Navarro X & Bostock H (2007). Velocity recovery cycles of single C fibres innervating rat skin. *J Physiol* **578**, 213–232.

Gokin AP, Philip B & Strichartz GR (2001). Preferential block of small myelinated sensory and motor fibers by lidocaine: in vivo electrophysiology in the rat sciatic nerve. *Anesthesiology* **95**, 1441–1454.

Gordon TR, Kocsis JD & Waxman SG (1990). Electrogenic pump (Na^+/K^+-ATPase) activity in rat optic nerve. *Neuroscience* **37**, 829–837.

Gover TD, Kao JP & Weinreich D (2003). Calcium signaling in single peripheral sensory nerve terminals. *J Neurosci* **23**, 4793–4797.

Hille B (1971). The permeability of the sodium channel to organic cations in myelinated nerve. *J Gen Physiol* **58**, 599–619.

Hodgkin AL & Katz B (1949). The effect of sodium ions on the electrical activity of the giant axon of the squid. *J Physiol* **108**, 37–77.

Jirounek P, Chardonnens E & Brunet PC (1991). After potentials in nonmyelinated nerve fibers. *J Neurophysiol* **65**, 860–873.

Jung HY, Mickus T & Spruston N (1997). Prolonged sodium channel inactivation contributes to dendritic action potential attenuation in hippocampal pyramidal neurons. *J Neurosci* **17**, 6639–6646.

Kobayashi J, Ohta M & Terada Y (1997). Evidence for the involvement of Na^+-K^+ pump and K^+ conductance in the post-tetanic hyperpolarization of the tetrodotoxin-resistant C-fibers in the isolated bullfrog sciatic nerve. *Neurosci Lett* **236**, 171–174.

Leffler A, Reiprich A, Mohapatra DP & Nau C (2007). Use-dependent block by lidocaine but not amitriptyline is more pronounced in tetrodotoxin (TTX) -resistant Nav1.8 than in TTX-sensitive Na^+ channels. *J Pharmacol Exp Ther* **320**, 354–364.

Mickus T, Jung H & Spruston N (1999). Properties of slow, cumulative sodium channel inactivation in rat hippocampal CA1 pyramidal neurons. *Biophys J* **76**, 846–860.

Morita K, David G, Barrett JN & Barrett EF (1993). Posttetanic hyperpolarization produced by electrogenic Na^+-K^+ pump in lizard axons impaled near their motor terminals. *J Neurophysiol* **70**, 1874–1884.

Ogata N & Tatebayashi H (1992). Slow inactivation of tetrodotoxin-insensitive Na^+ channels in neurons of rat dorsal root ganglia. *J Membr Biol* **129**, 71–80.

Orstavik K, Namer B, Schmidt R, Schmelz M, Hilliges M, Weidner C, Carr RW, Handwerker H, Jorum E & Torebjork HE (2006). Abnormal function of C-fibers in patients with diabetic neuropathy. *J Neurosci* **26**, 11287–11294.

Orstavik K, Weidner C, Schmidt R, Schmelz M, Hilliges M, Jorum E, Handwerker H & Torebjork E (2003). Pathological C-fibres in patients with a chronic painful condition. *Brain* **126**, 567–578.

Rang HP & Ritchie JM (1968). On the electrogenic sodium pump in mammalian non-myelinated nerve fibres and its activation by various external cations. *J Physiol* **196**, 183–221.

Raymond SA (1979). Effects of nerve impulses on threshold of frog sciatic nerve fibres. *J Physiol* **290**, 273–303.

Raymond SA, Thalhammer JG, Popitz-Bergez F & Strichartz GR (1990). Changes in axonal impulse conduction correlate with sensory modality in primary afferent fibers in the rat. *Brain Res* **526**, 318–321.

Renganathan M, Cummins TR & Waxman SG (2001). Contribution of $Na_v1.8$ sodium channels to action potential electrogenesis in DRG neurons. *J Neurophysiol* **86**, 629–640.

Roy ML & Narahashi T (1992). Differential properties of tetrodotoxin-sensitive and tetrodotoxin-resistant sodium channels in rat dorsal root ganglion neurons. *J Neurosci* **12**, 2104–2111.

Rush AM, Brau ME, Elliott AA & Elliott JR (1998). Electrophysiological properties of sodium current subtypes in small cells from adult rat dorsal root ganglia. *J Physiol* **511**, 771–789.

Rush AM & Elliott JR (1997). Phenytoin and carbamazepine: differential inhibition of sodium currents in small cells from adult rat dorsal root ganglia. *Neurosci Lett* **226**, 95–98.

Sandtner W, Szendroedi J, Zarrabi T, Zebedin E, Hilber K, Glaaser I, Fozzard HA, Dudley SC & Todt H (2004). Lidocaine: a foot in the door of the inner vestibule prevents ultra-slow inactivation of a voltage-gated sodium channel. *Mol Pharmacol* **66**, 648–657.

Schmidt R, Schmelz M, Forster C, Ringkamp M, Torebjork E & Handwerker H (1995). Novel classes of responsive and unresponsive C nociceptors in human skin. *J Neurosci* **15**, 333–341.

Senft JP (1967). Effects of some inhibitors on the temperature-dependent component of resting potential in lobster axon. *J Gen Physiol* **50**, 1835–1848.

Serra J, Campero M, Ochoa J & Bostock H (1999). Activity-dependent slowing of conduction differentiates functional subtypes of C fibres innervating human skin. *J Physiol* **515**, 799–811.

Shim B, Ringkamp M, Lambrinos GL, Hartke TV, Griffin JW & Meyer RA (2007). Activity-dependent slowing of conduction velocity in uninjured L4 C fibers increases after an L5 spinal nerve injury in the rat. *Pain* **128**, 40–51.

Spruston N, Schiller Y, Stuart G & Sakmann B (1995). Activity-dependent action potential invasion and calcium influx into hippocampal CA1 dendrites. *Science* **268**, 297–300.

Thalhammer JG, Raymond SA, Popitz-Bergez FA & Strichartz GR (1994). Modality-dependent modulation of conduction by impulse activity in functionally characterized single cutaneous afferents in the rat. *Somatosens Mot Res* **11**, 243–257.

Thomas RC (1972). Electrogenic sodium pump in nerve and muscle cells. *Physiol Rev* **52**, 563–594.

Townsend C & Horn R (1997). Effect of alkali metal cations on slow inactivation of cardiac Na^+ channels. *J Gen Physiol* **110**, 23–33.

Tripathi PK, Trujillo L, Cardenas CA, Cardenas CG, de Armendi AJ & Scroggs RS (2006). Analysis of the variation in use-dependent inactivation of high-threshold tetrodotoxin-resistant sodium currents recorded from rat sensory neurons. *Neuroscience* **143**, 923–938.

Vijayaragavan K, Boutjdir M & Chahine M (2004). Modulation of Nav1.7 and Nav1.8 peripheral nerve sodium channels by protein kinase A and protein kinase C. *J Neurophysiol* **91**, 1556–1569.

Weidner C, Schmelz M, Schmidt R, Hansson B, Handwerker HO & Torebjork HE (1999). Functional attributes discriminating mechano-insensitive and mechano-responsive C nociceptors in human skin. *J Neurosci* **19**, 10184–10190.

Weidner C, Schmidt R, Schmelz M, Hilliges M, Handwerker HO & Torebjork HE (2000). Time course of post-excitatory effects separates afferent human C fibre classes. *J Physiol* **527**, 185–191.

Weidner C, Schmidt R, Schmelz M, Torebjork HE & Handwerker HO (2003). Action potential conduction in the terminal arborisation of nociceptive C-fibre afferents. *J Physiol* **547**, 931–940.

Wood JN, Boorman JP, Okuse K & Baker MD (2004). Voltage-gated sodium channels and pain pathways. *J Neurobiol* **61**, 55–71.

Acknowledgements

We thank Jana Schramm, Maria Schulte and Birgit Vogler for their competent technical assistance. We are grateful to Christian Weidner and James Brock for their comments on the manuscript and also to Hugh Bostock for his suggestions regarding intracellular sodium. This work was supported by grants from the Deutsche Forschungsgemeinschaft (ME 995/1) and the Bundesministerium fuer Bildung und Forschung (BMBF German Headache Consortium).